Laser Interference Lithography for Applications in Biomedicine

W. Li[1,2], X. Wei[1], Q. Liu[1], D. Li[2] and Z. Wang[1,2]

[1] International Research Centre for Nano Handling and Manufacturing of China (CNM), Changchun University of Science and Technology, Changchun, China
[2]Institution for Research in Applicable Computing, University of Bedfordshire, Luton, UK

Abstract—**This paper presents a new maskless laser nanoscale manufacturing technology to fabricate micro and nano structured surfaces with specific functionalities. Cross-scale fabrication of micro and nano structures on biomaterials (such as metal, alloy and polyethylene) with wear resistant properties. Investigation of conditions and process parameters for cross-scale fabrication of micro and nano structures with specific functionalities (wear resistant properties) for the target applications in biomedicine.**

Keywords—**Laser interference lithography; Wear resistant; Biocompatibility; biomedicine**

I. Introduction

A lot of biomaterials can be used in the human body, such as metals (e.g. stainless steel, cobalt alloys, titanium alloys), ceramics (aluminium oxide, zirconia, calcium phosphates), and synthetic and natural polymers [1]. Since the focus of biomaterials has shifted towards medical implants, complex medical applications in biotechnology, it is significant to better define and evaluate the specific interaction between biomaterials and physiological surroundings [2-4]. All of these desirable functions of biomaterials are dependent on the mechanical, tribological and chemical properties of surfaces which can be controlled by surface modification technologies [5]. Numbers of surface modification technologies have been proposed such as plasma-surface modificaiton (PSM), chemical modification of materials, LIL, heat Treatment and coating techniques which will be introduced in the second sections.

This research focuses on developing LIL technologies for highly controllable, low cost and high efficiency manufacturing of micro and nano structured surfaces and components with proper functionanlities for applications in biomedicine. Coverage includes structure design, process control, and the characterisation of the modified surfaces. LIL can alter the surface compositions and properties of biomaterials in a well designed and highly controllable way, which makes them efficient and cost-effective tools for surface modification. The advantages of LIL for surface modification can be concluded as follows: high efficiency, low cost, highly controllable operation and various materials.

The laser energy distribution modulated by coherent beams is transferred to the material surface to produce the periodic structures directly by a high-power pulse laser. LIL offers its innovation to fabricate controllable micro and nano structures with defined patterns and functionalities on various materials. The structures on substrates can be fabricated by controlling LIL process parameters such as the incident angle, polarization direction, laser fluence and exposure time [6-7]. LIL has the advantage of fabricating micro and nano surface structures with different functionalities, compared with other traditional methods.

II. Principle

A. Laser interference lithography

In the case of the TE-TE-TM mode under the experimental conditions of three-beam interference, the intensity distribution I can be written as [8]

$$I = A^2 \left\{ \begin{array}{l} 3 + \sqrt{3}\cos\theta \cdot \cos(k \cdot \sin\theta \cdot y) \\ -\sqrt{3}\cos\theta \cdot \cos[k \cdot (\frac{\sqrt{3}}{2}\sin\theta \cdot y + \frac{3}{2}\sin\theta \cdot x)] \\ -\cos[k \cdot (\frac{\sqrt{3}}{2}\sin\theta \cdot y - \frac{3}{2}\sin\theta \cdot x)] \end{array} \right\} \quad (1)$$

Where A is the amplitude, θ is the incident angle, $k = 2\pi\lambda^{-1}$ is the wave number, and x and y are the coordinates.

The interference pattern of three beams can be calculated by Eq. (1). According to the principle of interference, when three coherent laser beams are superposed together, the light intensity in the interference field will be redistributed.

In laser interference lithography, matter melting, redeposition and re-crystallization processes occur. Ablation of surface is accompanied to local annealing, which could activate phase transitions in the laser-affected zone. The laser beam interaction plays a key role in heat propagation, which could result in the formation of modified material layers. Laser heating will cause variations in dislocation and residual stress distributions, formation of different carbide types, size and shape modification of austenitic grains and

H. Eskola et al. (eds.), *EMBEC & NBC 2017*,
IFMBE Proceedings 65,
DOI: 10.1007/978-981-10-5122-7_117

hardening effects [9]. It is known that the grain size is closely related to the hardness [10]. The influence of grain size on the hardness is usually expressed by the Hall-Petch relationship[11]:

$$H = H_0 + k_H d^{-1/2} \quad (2)$$

where d is the average grain size, H is the hardness, and H_0 and k_H are the material constants. It can be seen from the equations that the smaller grain size corresponds to the higher hardness.

B. Friction

The phenomenon of friction can be observed in many sliding and rolling situations, as a result of the action of various mechanisms at different levels. The main mechanisms of dry friction are adhesion, deformation, fracture, the ratchet, and third-body mechanisms [12]. Previous work shows that the friction coefficient is related to the factors such as the real contact area, contacting state and wear debris [13]. According to the adhesion and deformation model of friction, the dry friction coefficient μ can be expressed as [14]

$$\mu = \frac{A_r \tau_a + A_{ds} \tau_{ds} + A_{dp} \tau_{dp}}{W} \quad (3)$$

where W is the normal load, A_r, A_{ds}, and A_{dp} are the real areas of contact during adhesion, during two-body deformation and with particles, respectively, and τ is the shear strength.

The real area of contact is dependent on the surface topography, elastic modulus for elastic contact and hardness for plastic contact. The debris particles are formed during fretting and trapped in the contact zones. They play a significant role in the friction and wear processes in dry condition [15]. Particles trapped at the interface and hardness determine the real area of three-body contact [14]. Fig. 1 shows the schematic diagram of the lubrication model. Dimples increase the load-carrying capacity and the thickness of the joint lubricant film, which reduces the real contact area between the articulating surfaces. Under the dry condition, the abrasive wear particles being trapped in the dimples make the particle removal action will reduce friction and wear [16], which further improves the quality of artificial hip joints. The lubricant accumulated in the dimples can subsequently be dispensed during poor lubrication.

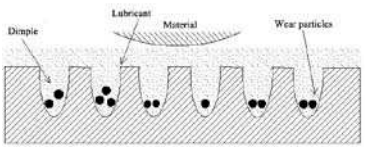

Fig. 1 Schematic of the lubrication model, reducing friction by the formation of dimples.

III. EXPERIMANT

Wear resisitance surfaces

In the experiment, highly-ordered dimple structures were fabricated by three-beam laser interference lithography. Co-Cr-Mo implant alloy samples were cut into cylindrical sections of about 2 mm long and 150 mm in diameter. All the samples were first polished in a grinder with the diamond polishing paste to achieve a mirror surface finish, and then patterned by laser interference lithography. A high power pulsed Nd:YAG laser with the wavelength of 1064 nm, frequency of 10 Hz, pulse energy of 2 J and pulse duration of 7-9 ns was used in the laser interference lithography system. The samples were processed with different exposure durations and laser fluences of interference beams. Each sample was cleaned with acetone and then rinsed in ethanol and deionized H_2O.

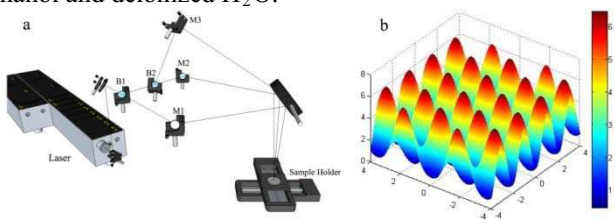

Fig. 2 (a) Schematic diagram of a three-beam interference setup and (b) 3D computer simulation result.

The experimental setup is shown in Fig. 2. The laser beams were split with beamsplitters and mirrors. Quarter wave plates and polarizers were placed before the exposed samples to select the power and polarization angles. The incident angles in the experiment were 5° and the laser fluence was $0.15 Jcm^{-2}$ or $0.26 Jcm^{-2}$. The spatial angle between incident beams was 120°. The three-beam laser interference lithography system was used to produce patterns with the structure period of $8 \mu m$. The laser output energy was measured with a laser power and energy meter. The surface morphology of the sample was examined by SEM. The RETC micro-friction and wear tester was used to analyze the friction properties of the surface with dry friction conditions. The 440C stainless steel ball (40 mm in diameter) was used as the dual pieces, and the reciprocating friction was measured. The friction testing conditions are shown in Table 1.

Table1. The friction testing conditions

Normal load (N)	Sliding speed (mm/S)	Single trip (mm)	Friction time (min)	Sampling frequency (Hz)	Temperature (℃)	Relative humidity (%)
3	0.5	3	5	5000	25	20

A micro-hardness tester (MH-60) was also used to measure the micro hardness of the modified surface. The applied

load for the indentation was set to 200 gf for a duration of 10 seconds at room temperature. Both untreated and modified samples were tested for comparison.

As a result of the high peak power of nanosecond laser source, the sample was patterned at a high temperature during exposure. Fig. 3 shows the SEM images of the sample surface after the exposure and hardness testing results. The laser fluence and exposure duration have a strong influence on the hardness properties. The depth of dimple and the heat diffusion are dependent on the laser fluence and exposure duration, and they will increase with the exposure duration. The heat diffusion will cause the increase of HAZ area and hardening region along with the sample distortion and alloy element vaporization. The longer the exposure duration is, the more the thermal diffusion process will extend in the Co-Cr-Mo alloy, enlarging the HAZ area and hardening region. The hardness of the dimpled and non-dimpled surfaces was measured by the MH-60 micro-hardness tester. Since the threshold of Co-Cr-Mo alloy ablation determines the energy of single laser pulses to be used, impacts of different fluences need to be investigated. The Vickers hardness indentation is shown in Fig. 3 (c). The samples with the laser fluences of $0.15 Jcm^{-2}$ and $0.26 Jcm^{-2}$ were chosen to analyze the effect on the HV with different exposure durations. Fig. 4 clearly shows that the sample surface modified with laser interference lithography has higher hardness compared with the untreated sample. The high hardness surface can be obtained with proper values of them.

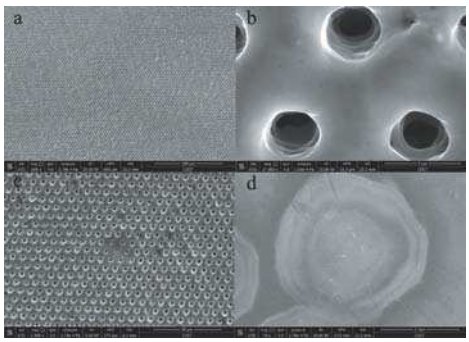

Fig. 3 (a) SEM image of the micro structure fabricated by three beam laser interference; (b) Close-up image of the micro structure; (c) SEM image of Vickers indentation with the load for the indentation 200 gf for a duration of 10 seconds; (d) The whole indentation pattern spot.

When the laser fluence increases further, the Vickers hardness (HV) will increase due to the increased heat input. The hardness of the grain refinement formed during the high temperature was increased in the laser-affected zone. This result suggests that the phase transition phenomena occurrence induced by laser heating, which is in agreement with the previously reported results [35].

Table 2 Test conditions with different exposure durations.

Samples	Exposure duration (s)	Fluences (Jcm-2)	Temperature (℃)	Conditions
1	0	0	25	Clean-room
2	30	0.26		
3	40	0.26		
4	50	0.26		
5	60	0.26		

The friction coefficient is an essential tribological quantity and a lower value is highly desirable for artificial joints. The tribological effects of various parameters with different exposure durations were investigated using a RETC micro-friction and wear tester under dry friction conditions. The test conditions with different exposure durations are shown in Table 2. The curves of Co-Cr-Mo alloy surface friction coefficients, as the experimental results, are shown in Fig. 5. Compared with the untreated samples, the results show that the friction coefficients are affected by the exposure duration.

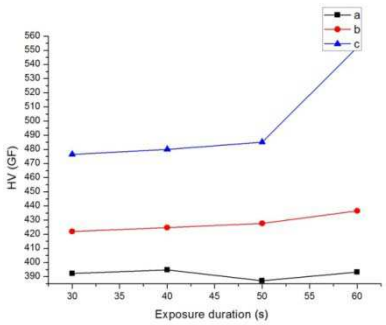

Fig. 4 The curves of Co-Cr-Mo alloy surface Vickers hardness: (a) Untreated sample; (b) Laser fluence of $0.15 Jcm^{-2}$; (c) Laser fluence of $0.26 Jcm^{-2}$.

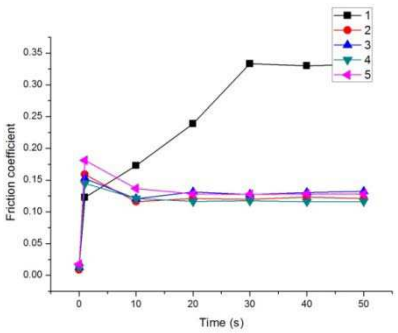

Fig. 5 The curves of Co-Cr-Mo alloy surface friction coefficients.

The friction coefficients of the untreated samples had a steep slope for the first 30 s. However, the sample surface modified with laser interference lithography had a slope for

the first 5 s in their respective "run-in" stages. Then both of the friction coefficients were in their stable stages. The stable friction coefficients at this stage were observed to be 0.33 and 0.12 for the untreated sample and the sample modified with laser interference lithography, respectively, indicating that they exhibited significantly differences. The modified sample with patterned microtextures exhibits extremely low friction coefficients. It is also found that the friction coefficients are increased with the exposure duration. That is because when the exposure duration exceeds a certain level, the structures are molten and destroyed.

IV. CONCLUSIONS

This research focused on the development of LIL for new applications in biomedicine on micro and nano scales. LIL was studied on fabrication of micro and nano surface patterns with well defined functionalities to modified materials which were widely used in biomedicine. The well designed micro and nano structures fabricated by LIL have shown an excellent performance on surface modification for biomaterials to achieve the wear resistance surfaces.

ACKNOWLEDGMENT

This work was supported by National Key Basic Research Program of China (973 Program No.2012CB326406), EU FP7 (ECROBOT No.318971; BIORA No.612641), China-EU H2020 (FabSurfWAR Nos.S2016G4501 and 644971), International Science and Technology Cooperation Program of China (No.2012DFA11070), National Natural Science Foundation Program of China (No.61176002, and No.11103047), Doctoral Program of Higher Education of China (No.20112216110002), Jilin Provincial Science and Technology Program (No.201115157, No.20110704, No.201215136 and No.20140414009GH), and Science and Technology Program of Changchun City (No.11KP04).

REFERENCES

1. A. Unsworth, Artificial joints. In An Introduction to the Bio-Mechanics of Joints and Joint Replacement (Eds D. Dowson and V. Wright). 1981, 134-139. (Mechanical Engineering Publications Limited, London).
2. S. Watari, K. Hayashi, J. Wood, P. Russell, P. Nealey, C. Murphy, and D. Genetos. Modulation of osteogenic differentiation in hMSCs cells by submicron topographically-patterned ridges and grooves. Biomaterials. 2012, 33, 128-136.
3. A. Ross, A. Jiang, M. Bastmeyer, and J. Lahann. Physical aspects of cell culture substrates: topography, roughness, and elasticity. Small, 2012, 8, 336-355.
4. T. Lu, Y. Qiao and X. Liu. Surface modification of biomaterials using plasma immersion ion implantation and deposition. Interface Focus. 2012, 2, 325-336.
5. T. Lu, Y. Qiao and X. Liu. Surface modification of biomaterials using plasma immersion ion implantation and deposition. Interface Focus. 2012, 2, 325-336.
6. D. Wang, Z. Wang, Z. Zhang, Y. Yue, D. Li, and C. Maple. Effects of polarization on four-beam laser interference lithography. Applied Physics Letters. 2013, 102, 081903-1-081903-5.
7. D. Wang, Z. Wang, Z. Zhang, Y. Yue, D. Li and C. Maple, Direct modification of silicon surface by nanosecond laser interference lithography. Applied Surface Science, 2013, 282, 67-72.
8. B. Chichkov, C. Momma, S. Nolte, F. Von Alvensleben and A. Tünnermann, Femtosecond, picosecond and nanosecond laser ablation of solids. Applied Physics A, 1996, 63, 109-115.
9. E. Gualtieri, A. Borghi, L. Calabri, N. Pugno and S. Valeri, Increasing nanohardness and reducing friction of nitride steel by laser surface texturing. Tribology International, 2009, 42, 699-705.
10. M. Furukawa, Z. Horita, M. Nemoto, R. Valiev and T. Langdon, Microhardness measurements and the Hall-Petch relationship in an Al-Mg alloy with submicrometer grain size. Acta Materialia, 1996, 44, 4619-4629.
11. P. Bazarnik, Y. Huang, M. Lewandowska and T. G. Langdon, Structural impact on the Hall-Petch relationship in an Al-5Mg alloy processed by high-pressure torsion. Materials Science and Engineering: A, 2015, 626, 9-15.
12. M. Nosonovsky and B. Bhushan, Biologically inspired surfaces: broadening the scope of roughness, Advanced Functional Materals, 2008, 18(16), 843–855.
13. M. Varenberg, G. Halperin, and I. Etsion, Different aspects of the role of wear debris in fretting wear. Wear: an international journal on the science and technology of friction lubrication and wear, 2002, 252, 902-910.
14. B. Bhushan and M. Nosonovsky, Scale effects in dry and wet friction, wear, and interface temperature. Nanotechnology, 2004, 15, 749-761.
15. N. Diomidis and S. Mischler, Third body effects on friction and wear during fretting of steel contacts. Tribology International, 2011, 44, 1452-1460.
16. T. Hu and L. Hu, The study of tribological properties of laser-textured surface of 2024 aluminium alloy under boundary lubrication. Lubrication Science, 2012, 24, 84-93.

Author: Zuobin Wang
Institute: International Research Centre for Nano Handling and Manufacturing of China (CNM), Changchun University of Science and Technology, Changchun, China
Street: 7089 Weixing Road
City: Changchun
Country: China
Email: wangz@cust.edu.cn